3.2 LOW ACTIVATION JOINING OF SiC/SiC COMPOSITES FOR FUSION APPLICATIONS: MODELING MINIATURE TORSION TESTS WITH ELASTIC AND ELASTIC-PLASTIC MODELS — C.H. Henager, Jr., B.N. Nguyen, and R.J. Kurtz; (Pacific Northwest National Laboratory, Richland, WA, USA); M. Ferraris, (Politecnico di Torino, Torino, Italy); Y. Katoh, (Oak Ridge National Laboratory, Oak Ridge, TN, USA)

OBJECTIVE

Mechanics damage models have been developed to match torsion experiments involving elastic and elastic-plastic materials and to help formulate a path forward with joint testing and analysis for SiC materials in nuclear environments. This report extends the analysis from the last reporting cycle by including plots of stress fields and strain energy density fields and by limiting the model to shear damage.

SUMMARY

The international fusion community designed miniature torsion specimens for joint testing and irradiation in test reactors with limited irradiation volumes since SiC and SiC-composites used in fission or fusion environments require joining methods for assembling systems. Torsion specimens fail out-of-plane when joints are strong and when elastic moduli are comparable to SiC, which causes difficulties in determining shear strengths for many joints or for comparing unirradiated and irradiated joints. A finite element damage model was developed to treat elastic joints such as SiC/Ti_3SiC_2+SiC and elastic-plastic joints such as SiC/epoxy and steel/epoxy. The model uses constitutive shear data and is validated using epoxy joint data. The elastic model indicates fracture is likely to occur within the joined pieces to cause out-of-plane failures for miniature torsion specimens when a certain modulus and strength ratio between the joint material and the joined material exists. Lower modulus epoxy joints always fail in plane and provide good model validation.

PROGRESS AND STATUS

Introduction

The international fusion materials community is currently irradiating several joint types and compositions in the HFIR reactor at ORNL [1]. PNNL is working with Politecnico di Torino (POLITO) and ORNL using miniature torsion specimens (hourglass samples) that have been specifically designed for pre- and post-irradiation joint shear strength testing [2]. Many of the joints fail out-of-plane, or in the base CVD-SiC material, during torsion testing, but some do not. To elucidate how and where cracks can initiate and propagate in the torsion joint specimens, finite element analyses of these specimens subjected to torsion were performed using a continuum damage mechanics (CDM) model previously developed at PNNL for elastic materials for which any nonlinearity in stress/strain response is due solely to damage and not to other irreversible processes such as plasticity [3]. The CDM model was implemented in the ABAQUS® finite element code via user subroutines. Comparative analyses of the torsion joints using ABAQUS® and the damage model were conducted considering typical mechanical properties in shear of CVD-SiC and different mechanical behaviors of the joint material using assumed shear stress/strain responses up to failure. Since SiC/epoxy and steel/epoxy joints were used to validate the miniature torsion specimen design, a CDM elastic-plastic model is included.

Model Formulation

Approach

This section summarizes the damage model and method for predicting crack initiation and propagation [3-5] in the joined CVD-SiC or steel material together with a thin joint region consisting of either Ti_3SiC_2/SiC of varying modulus and strength or a hypothetical brittle epoxy and an elastic-plastic epoxy. Considering damage in an elastic and damageable material, for which any nonlinearity in stress/strain response is due solely to damage and not to other irreversible processes, can be described by a scalar variable, D, that can be related to the microcrack density or microcrack volume fraction, or simply a parameter to phenomenologically quantify the level of damage accumulation in the material [4]. Damage affects the material stiffness according to a stiffness reduction law. Using the concepts of thermodynamics of continuous media [4, 6], a thermodynamic potential is defined to derive the constitutive relations and the thermodynamic force associated with the damage variable. This damage model uses the density of the

elastic deformation energy as the thermodynamic potential that provides a coupling between damage and elasticity. A damage criterion dependent on a damage threshold function is defined and the damage evolution law is obtained. Damage evolves with the deformation according to the damage evolution law until a critical (saturation) state at which $D = D_{cr}$ $(0 < D_{cr} < 1)$ and failure occurs. D_{cr} is small for brittle materials, and this is the case for ceramic materials studied in this work. In this work, failure at damage saturation ($D = D_{cr}$) leading to crack initiation and propagation is modeled by a vanishing finite element technique [7] that reduces the stiffness and stresses of the failed element to zero [3, 8].

We choose to implement the damage model for brittle ceramics in shear loading (Figure 1a). In this case, a flaw under Mode III loading experiences some damage accumulation prior to critical crack growth due to frictional forces on the crack faces and a non-linear shear stress-strain curve results [9]. Furthermore, it is understood that this problem can be addressed using multiaxial loading considerations if a known flaw distribution was available [9-14], but that this is not practicable here. Rather, the damage model approach is used in a phenomenological sense to address the effects of load sharing in this complex joined system. The thermodynamic and CDM approach adopted is phenomenological. It does not describe the detailed frictional sliding of crack ligaments but the magnitude and effect of shear damage on the material response are *phenomenologically* captured by the damage variable, *D,* driven by the associated thermodynamic force, *F*(*D*), and the damage evolution law.

As discussed in Refs. [15, 16] miniature torsion joints were made at POLITO using Araldite AV119 epoxy between CVD-SiC and a 316-grade stainless steel. The epoxy was cured for 1 h at 130°C [15]. The torsion tests for these samples were performed in the same manner as all the other torsion testing. In addition, simple compression tests were performed [16] on cylinders of cured AV119 epoxy to establish the mechanical properties of this toughened adhesive material [17, 18]. Materials such as 316SS and AV119 epoxy exhibit pronounced nonlinear behaviors controlled by plasticity and damage. Therefore, an elastic-plastic damage description is used in this work to model the nonlinear responses of these materials to monotonic loading up to failure [19]. This elastic-plastic damage model was implemented in ABAQUS via user subroutines to describe the constitutive behaviors of the AV119 joint [18] and of the joined 316SS material [20] in the ABAQUS analyses of torsion specimens. Figs. 1b-c show the uniaxial stress/strain curves of 316SS and AV119 captured by this elastic-plastic damage model.

RESULTS

Model Results

The damage models are implemented in ABAQUS® as a finite element analysis of the miniature torsion joint specimen. In order to investigate specimen failure for different types of joints, different material properties of the joints were considered and are reflected through the assumed shear stress/strain responses up to failure in the damage models. In addition, typical mechanical properties of CVD-SiC and nominal steel (316SS) as the joined halves in the experimentally observed range were assumed. Figure 1 and Table 1 present the mechanical properties assumed in this parametric study. There are 5 different behaviors (denoted by case study numbers 1 through 5) considered for the Ti_3SiC_2/SiC composite joint differentiated by their calculated modulus and assumed failure strength. In addition, a similar analysis was performed for two epoxy joined CVD-SiC and steel specimens. The damage variable value at saturation was taken to be 0.2 for all the ceramics while it was considered to be 0.4 for the brittle epoxy (case 6) leading to an epoxy strength of 120 MPa and failure strain of 0.02 and 0.48 for an elastic-plastic epoxy (AV119, case 7) with a strength of 80 MPa at 0.05 failure strain [15, 16, 18].

Damage analyses were conducted for all the torsion joint specimens made of the simulated materials listed in Table 1, which are based on the calculated modulus values for the various joints with differing amounts of porosity. The predicted failure patterns for all the studied elastic cases are gathered in Figure 2. Computed stress and strain fields, along with the strain energy density field, for Case 1 are shown in Figure 3 to illustrate fields that are not related to the damage model. Cases 1 and 5 for the Ti_3SiC_2/SiC joint represent the extreme cases for the most dense joint in Case 1 and the least dense joint in Case 5. The failure location changes from within the CVD-SiC joined materials (Case 1) to within the joint plane (Case 5). Cases 2 and 3 represent Ti_3SiC_2/SiC joints made at 30 MPa and 20 MPa, respectively, which are increasingly less stiff than the joined CVD SiC. For both of these cases, failure is predicted to initiate in the joint but then develop into the SiC sample resulting in out-of-plan failure. Case 4 for the 10 MPa

Ti_3SiC_2/SiC joint is now only about 1/3 as stiff as the CDV-SiC and the simulation indicates a mixture of failure within the joint and within the sample. Experimentally, these 10 MPa joints sometimes fail within the joint and sometimes within the CVD-SiC. Case 5 is predicted to fail within the joint and experiments confirm this failure mode. The brittle epoxy joint (Case 6) also always exhibits in-plane failure.

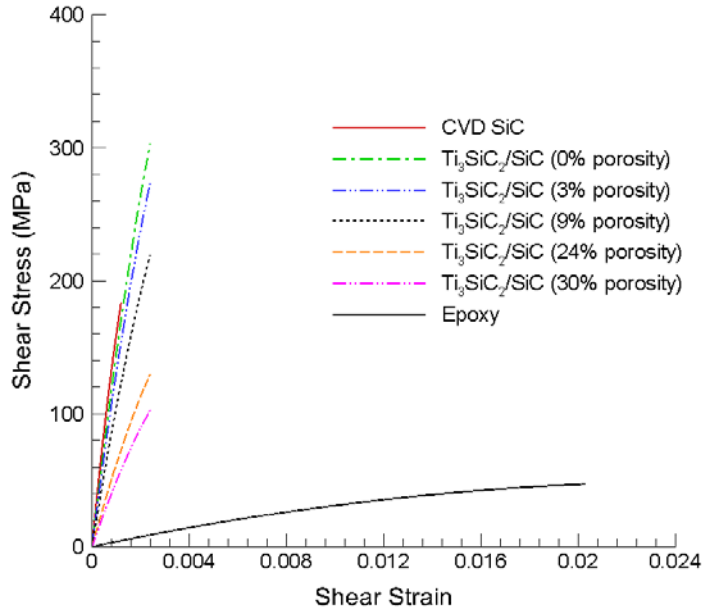

(a)

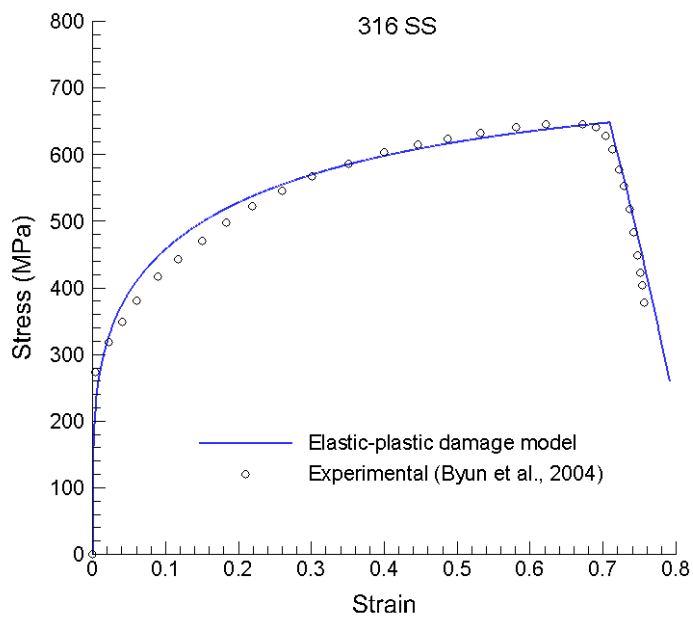

(b)

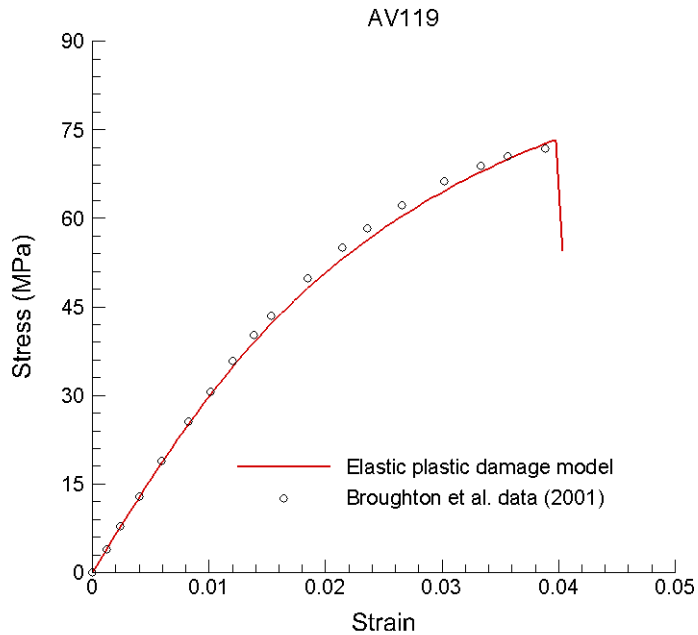

(c)

Figure 1. Shear and uniaxial stress/strain responses considered for (a) an elastic damage model for CVD-SiC and different types of joint material, including a brittle epoxy, (b) an elastic-plastic damage model for 316SS [20] and (c) an elastic-plastic damage model for AV119 epoxy [18]. See Tables 1 and 2 for model parameters.

Table 1. Mechanical properties of the CVD-SiC and joint material assumed for the analysis.

Material	Case Study No.	Shear Modulus (GPa)	Poisson Ratio	Shear Strength (MPa)	Failure Strain in shear	Damage Variable Critical Value
CVD-SiC	–	192	0.2	184	1.2×10^{-3}	0.2
Ti_3SiC_2+SiC (0% porosity)	1	158	0.2	304	2.4×10^{-3}	0.2
Ti_3SiC_2+SiC (3% porosity)	2	143	0.2	274	2.4×10^{-3}	0.2
Ti_3SiC_2+SiC (9% porosity)	3	115	0.2	220	2.4×10^{-3}	0.2
Ti_3SiC_2+SiC (24% porosity)	4	68	0.2	130	2.4×10^{-3}	0.2
Ti_3SiC_2+SiC (30% porosity)	5	54	0.2	103	2.4×10^{-3}	0.2
Epoxy (Brittle)	6	3.8	0.3	47	2.0×10^{-2}	0.4

Table 2. Parameters of the elastic-plastic models identified for 316SS and AV119.

Materials	E (MPa)	σ_0 (MPa)	v	n	$\bar{\varepsilon}_p^D$	$\bar{\varepsilon}_p^R$	D_c
316SS	193000	150	0.3	4.3	0.02	0.42	0.7
AV119	3200	110	0.34	3	0	0.01	0.45

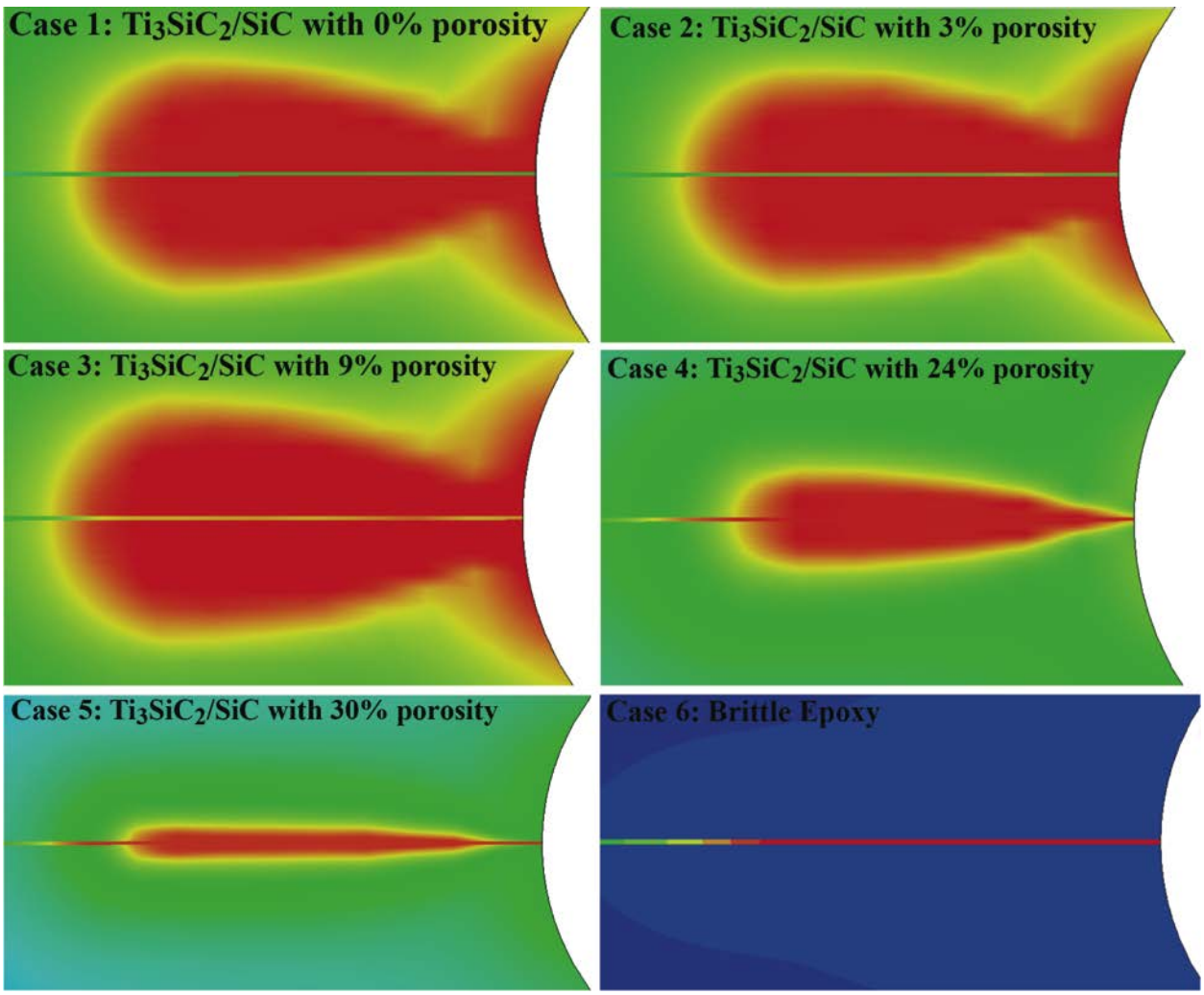

Figure 2. Predicted fracture patterns (red regions) using an elastic damage model for the torsion joint specimens made of different joint materials with mechanical properties listed in Table 1. Cases 1, 2, and 3 fail within the CVD-SiC base material (out-of-plane), while case 4 sometimes fails within the joint. Case 5 always fails in the joint region. Case 6 shows results from the brittle epoxy simulation, which also fails within the joint without exception.

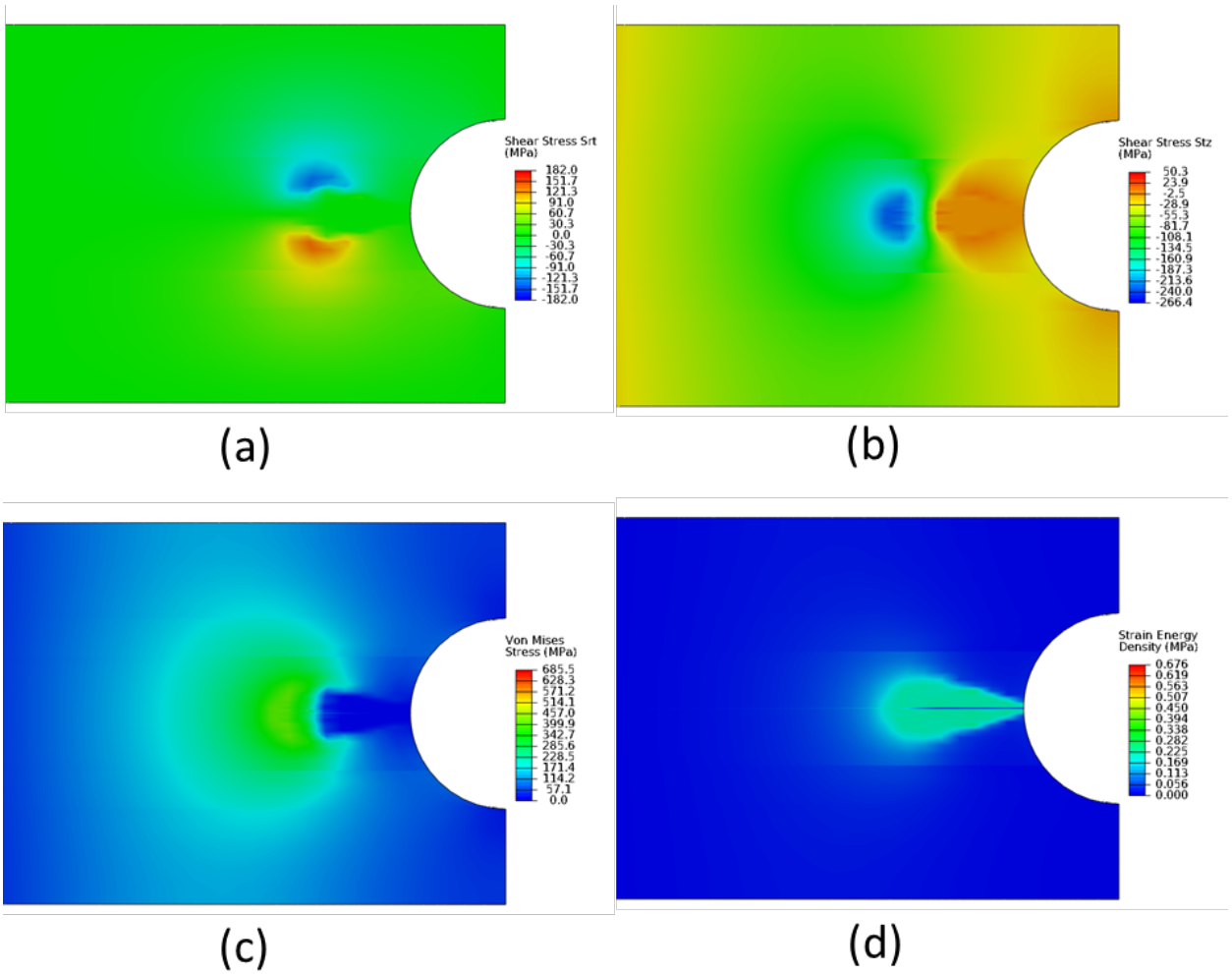

Figure 3. Contours of (a) shear stress τ_{rt}, (b) shear stress τ_{tz}, (c) equivalent Von Mises stress, and (d) strain energy density causing damage and fracture of Case 1 torsion joint specimen.

As recognized by Ferraris et al. [16] the toughened adhesive epoxy AV119 is not a brittle material but behaves as an elastic-plastic material and, therefore, must be treated accordingly. Figures 1b-c and Table 2 together with the elastic-plastic damage model provide the necessary tools to address this issue. In addition to using an elastic-plastic response, the joint thickness in the model was modified to more closely simulate the work performed in Torino. Figure 4 shows the predicted failure locations for a 50-µm thick AV119 joint between CVD-SiC and 316SS. The CVD-SiC is treated elastically as before but in this case the AV119 and 316SS are treated using the elastic-plastic model developed here. The model results validate what the torsion testing observed, namely, that the torsion specimens fracture in the plane of the joint when bonded using AV119 adhesive epoxy regardless of the specimen material.

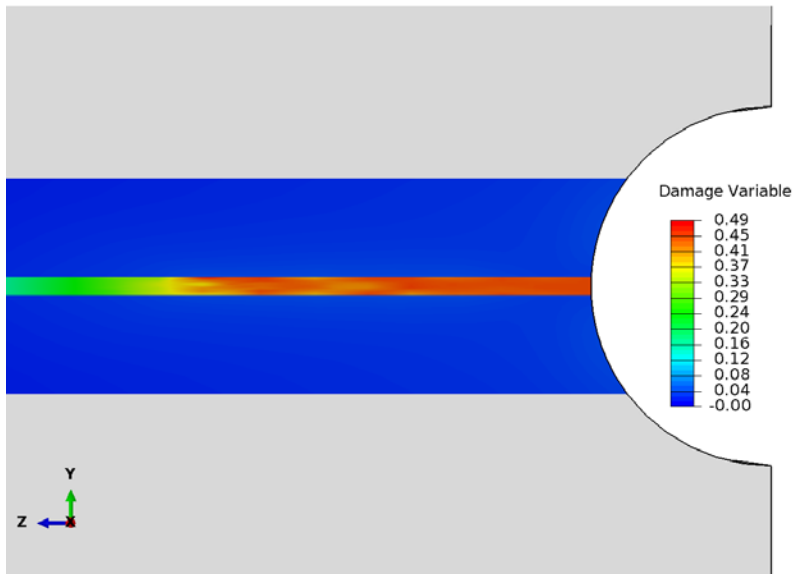

(a)

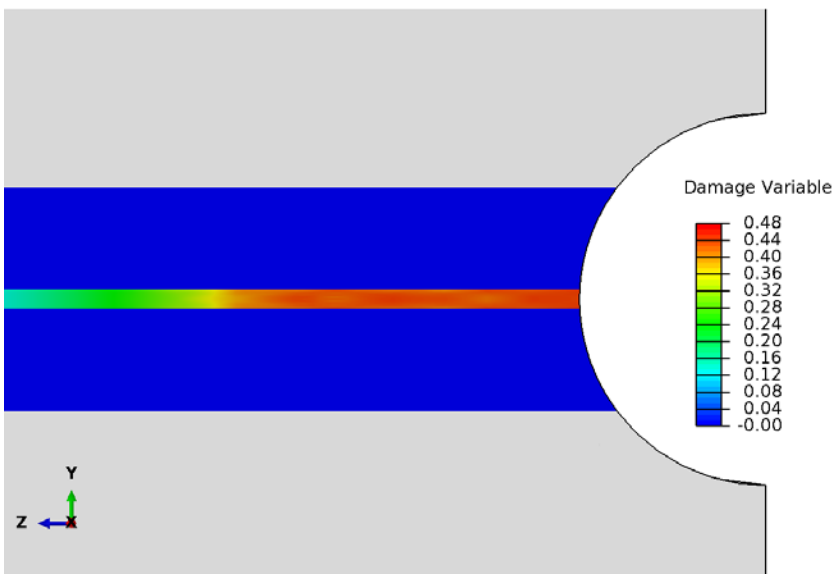

(b)

Figure 4. Predicted fracture patterns using an elastic-plastic damage model for the AV119 adhesive epoxy and for 316SS. Shown in (a) is the predicted fracture for CVD-SiC joined with AV119 where the epoxy is elastic-plastic and the SiC is elastic. Shown in (b) is the case for both materials obeying the elastic-plastic damage model for 316SS joined with AV119 epoxy. In all cases the failure occurs within the epoxy joint.

Discussion

Model Predictions and Comparisons

The damage models were created to help understand the fracture results from the THG specimens that exhibited non-planar fracture that was not truly reflective of joint properties. Rather, the literature refers to this data as “torsional shear resistance” of the THG [1, 2, 21-24] when the THG specimen fails in the base material, or out-of-plane. The critical part of the damage models was to be able to simulate the stress-

strain curves for the constitutive materials; otherwise the models would not be reasonable. The shear stress-strain curves shown in Figure 1a using the data in Table 1 capture the material elastic constants as well as the failure strengths and are reasonable assumptions. In addition, the stress-strain responses computed by the elastic-plastic damage model shown in Figures 1b and c correctly capture the stress-strain behavior of both the 316SS steel and AV119 epoxy. The accuracy of the THG damage modeling is predicated on the accuracy of the individual constituent's stress-strain data and, even though this model data is not completely precise, the results from carefully applying the model are expected to show the desired effects.

The models, both the elastic damage and elastic-plastic damage approaches, capture the key observations, namely that there is a transition from planar to non-planar fracture over a range of elastic moduli and strength values. High strength and high moduli materials are predicted to fail out-of-plane and within the base THG material, whereas low modulus materials fail in the plane of the joint. Intuitively, it is anticipated that low modulus epoxy will behave differently compared to high modulus Ti_3SiC_2+SiC or CA glass-ceramic in terms of load sharing with the CVD-SiC base material. In fact, one thought (*gedanken*) experiment is to imagine the entire miniature torsion specimen machined from a single piece of CVD-SiC and then to predict where it will fail. Probabilistic brittle fracture mechanics predicts that it will fail somewhere in the specimen that contains a combination of the largest flaw and the highest tensile/shear stresses, which will not necessarily coincide with the central plane of the torsion specimen. Thus, a high strength, high modulus joint may not fail in the plane of the joint either. As shown in Figs. 2 and 3 load sharing with the CVD-SiC forces a majority of the damage for high modulus joints to occur within the base CVD-SiC material and failure is predicted to occur out-of-plane of the joint. However, this load sharing is a function of the constitutive behavior (i.e., modulus, stress-strain response, etc.) differences between the joint and base THG material. The model predicts a high degree of load sharing and CVD-SiC damage for a joint modulus greater than about 200 GPa and a minimal amount of load sharing with highly localized (planar) fracture for moduli 100 GPa and lower (Figure 2). This is in good agreement with the observed experimental data for the THG joints tested at POLITO (Figure 5).

Figure 5a shows the computed maximum shear stresses for all the cases studied in this work. The maximum shear stress is highest (104 MPa) for the specimen with the Ti_3SiC_2+SiC stiffest and strongest joints, cases 1, 2, and 3. Cases 4 and 5 have shear strengths that are smaller than this and, in the simulation, reflect the shear strength of the joint. In addition, the predicted failure strengths in shear shown in Figure 5a correlate with measurements from ORNL and POLITO [1, 21]. The ORNL data for the unirradiated Ti_3SiC_2+SiC joints indicated a torsional shear resistance value of 117 MPa ± 10 MPa, which agrees with the model prediction of 104 MPa [1]. It is noted that this predicted strength value follows from the CVD-SiC damage model determined from the *assumed* CVD-SiC mechanical properties. Thus, the model predicts that the torsion test will fail in the CVD-SiC material and that the torsional shear resistance of the sample will be 104 MPa because that is the predicted shear strength of the CVD-SiC simulated here. Note that the NITE materials tested in Ref. [1] fail at higher shear strengths compared to the CVD-SiC and this is attributed to the higher shear strength of the NITE SiC. However, the main point is that for certain material combinations the THG test will fail at the shear strength limit of the base material and will not provide information regarding the shear strength of the joint material.

The epoxy joined data from POLITO is more complex. Results indicate a shear fracture strength of 36 MPa, which agrees with the model prediction of about 38 MPa[1] for the brittle epoxy material (Case 6 and Figure 5a). In this case, where the epoxy modulus is only a fraction of the CVD-SiC or 316SS the fracture path is in the plane of the joint in the epoxy material and provides a true shear stress value. However, since AV119 toughened adhesive epoxy is not a linear elastic brittle material, the elastic damage model is not appropriate and an elastic-plastic damage model was developed based on mechanical property data for AV119 and 316SS as discussed. This model predicts a shear failure strength of 28 MPa for a 50-µm thick joint region of AV119 (Figs. 5a and 5b), which is less than the POLITO calculated value of 36 MPa but is in agreement with the measured asymmetric 4-point bending for epoxy-joined SiC [16]. However, Ferraris et al. also report a value of 66 MPa ± 10 MPa for AV119-joined THG CVD-SiC specimens where the shear strength is calculated using $\tau = k\frac{16\,T}{\pi d^3}$, where T is the applied torque and d is the minimum

[1] Personal Communication from Prof. M. Ferraris of Politecnico di Torino. They used AV119 Epoxy with an elastic modulus of 2.8 GPa and Poisson ratio of 0.4. They obtained accurate, in-plane shear failures for all tests and a shear strength of 36 MPa ± 8 MPa.

radius at the fillet of the miniature torsion specimen, and *k* was set to 1. However, as discussed in Timoshenko and Goodier [25] this equation is only strictly valid for linear elastic homogeneous bodies, not for elastically dissimilar bodies, and *k* for the miniature torsion specimen is not equal to 1. In addition, applying this equation for elastic-plastic materials is inappropriate as discussed in Ref. [16]; rather it is suggested that this value be reduced and a value of 36 MPa is suggested as a more accurate value, which is in general agreement with the FE model results presented here of 28 MPa. This model prediction is based solely on the accuracy of the assumed mechanical properties of AV119 adhesive epoxy taken from Ref. [18], however the strength of AV119 depends on the curing time and temperature, etc., so that the value determined by the elastic-plastic model here might differ from AV119 experimental data.

Data Interpretation and Torsion Test Future

Since the model predicts that high strength, high modulus joints will likely not fail so as to provide a true shear strength for the joints then an obvious point of discussion is what to make of the miniature torsion test? First, the THG specimen is ideal for small-volume, in-reactor experiments and provides a vehicle for obtaining valuable microstructural evolution data for experimental joints. The THG specimen can still provide microstructural evolution leading to differential strains, environmental exposures, and radiation damage. This became clear in the HFIR data recently obtained at ORNL [1]. In that respect, the miniature THG specimen is a successful design.

Second, changes in joint strength or moduli due to radiation damage can be revealed during post-irradiation joint testing. The Ti_3SiC_2+SiC joints survived after 800˚C (1073 K) and 5 dpa but the torsion failure location changed from CVD-SiC base material failure to in-plane joint failure as noted in Ref. [1]. This suggests that a major change occurred in the joined specimens and post-irradiation microscopy revealed interface cracking and microcracking within the joint material. This is thought to be due to either thermal expansion or swelling mismatches between the joint material and the CVD-SiC and/or within the dual-phase joint material. Thus, both shear strength and shear failure location can be used to help understand joining for fusion materials. The model can guide experimental data interpretation by allowing various parameters to be controlled and varied. Many of these parameters can be independently quantified so that the model can be refined as needed.

The torsion shear test is an example of a seemingly simple mechanical test that is, in reality, a complex multiaxial loading problem and methods exist to address these problems in terms of strengths and failure probabilities [9-14]. For future reference, if flaw distributions were known for CVD-SiC and for the joint materials, plus flaws at the joint/CVD-SiC interface, then a true multiaxial, probabilistic solution to the THG specimen could be implemented. However, such an approach is outside of the scope of this study and would be extremely challenging to implement since determining the actual flaw distributions would be a difficult task. Still, the transition from out-of-plane, base CVD-SiC failure to in-plane joint failures that was observed in the post-irradiation testing of these joints most likely indicates a change in the joint flaw distribution due to the irradiation exposure. Significantly, new flaws were observed in post-irradiation SEM examinations of these joints [1].

Finally, it is noted that for a THG specimen previously subjected to neutron irradiation, the experimentally determined irradiated elastic properties can be used to compute the initial elastic stiffness of the irradiated material, and knowing thermal expansion coefficients, thermal stresses can be computed that represent the residual stresses before any mechanical actions (i.e., applied torsion loading). Exactly the same kind of FE analysis of the THG specimen can be applied to elucidate how important the contribution of residual stresses is on the onset of cracking, crack propagation, and shear strength of the irradiated THG specimen. This manuscript does not address the effects of residual stress or the effects of neutron damage, such as differential swelling leading to irradiation-induced stresses, even though it is anticipated that these will be significant, since at this time these effects are not known with certainty for any of these joined material combinations. This level of detail can certainly be implemented in the model presented here but will be reserved for a future study.

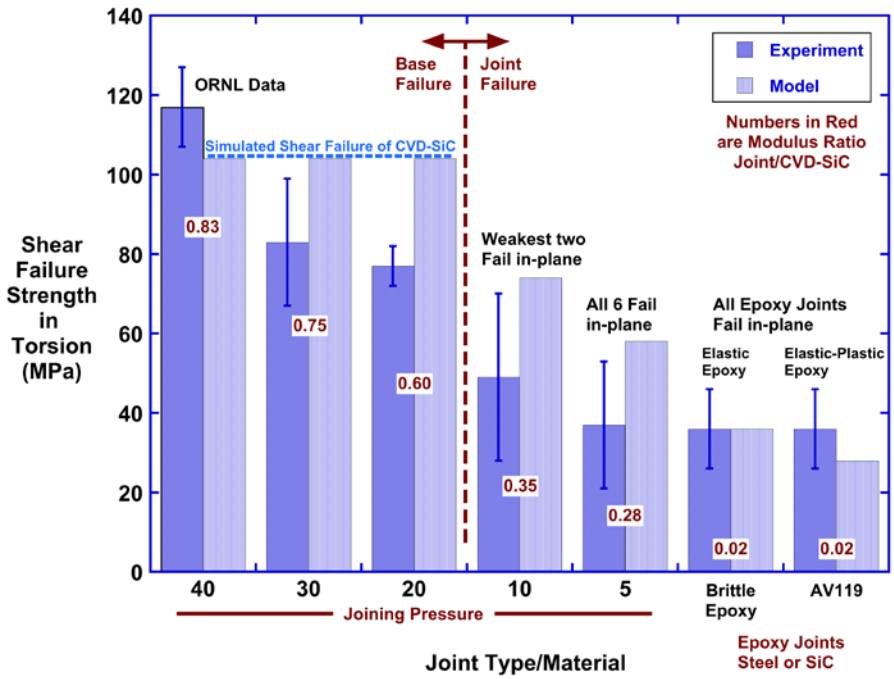

(a)

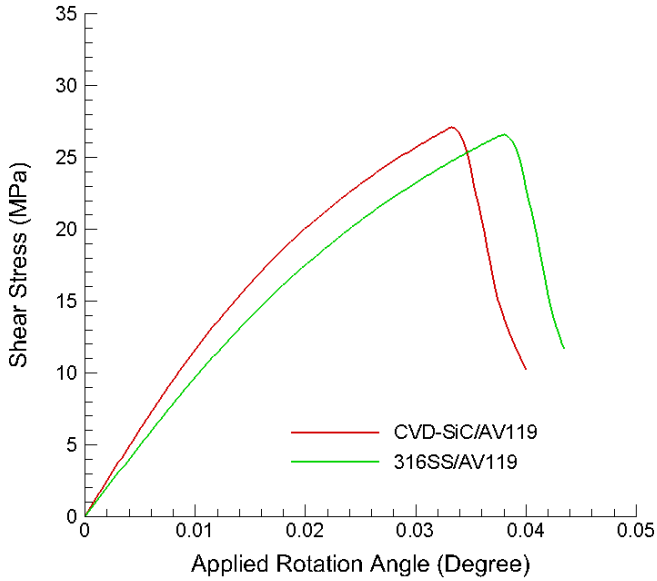

Figure 5. Shown in (a) is the predicted maximum shear stress at fracture for all damage model simulations together with experimental data. Shown in (b) is the predicted evolution of the maximum in-plane shear stresses with applied rotation angle for the elastic-plastic AV119 cases from Figure 4.

Future Work

The in-reactor irradiation results from ORNL display a failure mechanism that is not included in the model yet, namely, the failure of the joint/CVD-SiC interface. Both the Ti_3SiC_2+SiC joints and the CA glass-ceramic joints exhibited interface fractures located at the joint/CVD-SiC interface. The model assumes a

strongly bonded interface between the joint and CVD-SiC and no evolution of that bond is treated in the FE model. Future model implementations will treat the interface as a separate material region with an identifiable strength.

Acknowledgements

This research was supported by Office of Fusion Energy Sciences, U.S. Department of Energy (DOE) under Contract DE-AC05-76RL01830.

References

[1] Katoh, Y., L.L. Snead, T. Cheng, C. Shih, W.D. Lewis, T. Koyanagi, T. Hinoki, C.H. Henager Jr, and M. Ferraris, J. Nucl. Mater., (2014), 448(1-3), 497-511.
[2] Jung, H.-C., T. Hinoki, Y. Katoh, and A. Kohyama, J. Nucl. Mater., (2011), 417(1-3), 383-386.
[3] Nguyen, B.N., B.J. Koeppel, S. Ahzi, M.A. Khaleel, and P. Singh, J. Am. Ceram. Soc., (2006), 89(4), 1358-1368.
[4] Lemaitre, J. and J.L. Chaboche, Journal de Mecanique Appliquee, (1978), 2(3), 317-65.
[5] C. H. Henager, J., B.N. Nguyen, R.J. Kurtz, T. Roosendaal, B. Borlaug, M. Ferraris, A. Ventrella, and Y. Katoh, in Fusion Reactor Materials Program Semiannual Progress Reports, Vol. 56, F. Wiffen, R. Godfrey, and B. Waddell, Editors,(2014), ORNL: Oak Ridge, TN, p. 79-93.
[6] Maugin, G.A., The Thermomechanics of Plasticity and Fracture. (1992), Cambridge, UK: Cambridge University Press.
[7] Tvergaard, V., Int. J. Fract., (1986), 31(3), 183-209.
[8] Nguyen, B.N., V. Kunc, J.H. Phelps, C.L. Tucker Iii, and S.K. Bapanapalli, in 23rd Technical Conference of the American Society for Composites (2008), September 9, 2008 - September 11, 2008, Memphis, TN, United states: DEStech Publications Inc.
[9] Chao, L.-Y. and D.K. Shetty, J. Am. Ceram. Soc., (1990), 73(7), 1917-1921.
[10] Nemeth, N.N., Int. J. Fract., (2014), 185(1-2), 97-114.
[11] Fett, T., D. Munz, and G. Thun, J. Am. Ceram. Soc., (2003), 86(8), 1427-1429.
[12] Suresh, S., C.F. Shih, A. Morrone, and N.P. O'Dowd, J. Am. Ceram. Soc., (1990), 73(5), 1257-1267.
[13] Lamon, J., J. Am. Ceram. Soc., (1990), 73(8), 2204-2212.
[14] Priddle, E.K., Journal of Strain Analysis, (1969), 4(2), 81-87.
[15] Ferraris, M., M. Salvo, V. Casalegno, M. Avalle, and A. Ventrella, Int. J. Appl. Ceram. Technol., (2012), 9(4), 795-807.
[16] Ferraris, M., A. Ventrella, M. Salvo, and D. Gross, Int. J. Appl. Ceram. Technol., (2014), 11(2), 394-401.
[17] Xu, B., "Fracture Mechanisms and Failure Criteria of Adhesive Joints and Toughened Epoxy Adhesives," in School of Engineering and Materials Science. (2010), Queen Mary, University of London: University of London, p. 225.
[18] Broughton, W.R., L.E. Crocker, and J.M. Urquhart, "Strength of Adhesive Joints: A Parametric Study," (2001), T. National Physical Laboratory, Middlesex, TW11 0LW, UK, NPL Materials Centre, National Physical Laboratory, Teddington, Middlesex, TW11 0LW, UK, p. 41.
[19] C. H. Henager, J., B.N. Nguyen, R.J. Kurtz, T. Roosendaal, B. Borlaug, M. Ferraris, A. Ventrella, and Y. Katoh, in Fusion Reactor Materials Program Semiannual Progress Reports, Vol. 57, F. Wiffen, R. Godfrey, and B. Waddell, Editors, (2014), ORNL: Oak Ridge, TN, p. 74-84.
[20] Byun, T.S., N. Hashimoto, and K. Farrell, Acta Mater., (2004), 52(13), 3889-3899.
[21] Ferraris, M., A. Ventrella, M. Salvo, Y. Katoh, and D. Gross, Int. J. Appl. Ceram. Technol., (2014), in press.
[22] Hinoki, T., Y. Katoh, L.L. Snead, H.-C. Jung, K. Ozawa, H. Katsui, Z.-H. Zhong, S. Kondo, Y.-H. Park, C. Shih, C.M. Parish, R.A. Meisner, and A. Hasegawa, Mater. Trans., (2013), 54(4), 472-476.
[23] Ferraris, M., M. Salvo, S. Rizzo, V. Casalegno, S. Han, A. Ventrella, T. Hinoki, and Y. Katoh, Int. J. Appl. Ceram. Technol., (2012), 9(4), 786-794.
[24] Ferraris, M., M. Salvo, V. Casalegno, S. Han, Y. Katoh, H.C. Jung, T. Hinoki, and A. Kohyama, J. Nucl. Mater., (2011), 417(1-3), 379-82.
[25] Timoshenko, S.P. and J.N. Goodier, Theory of Elasticity, Third ed. Engineering Societies Monographs. (1970), New York: McGraw Hill.